

Calibrated Intervention and Containment of the COVID-19 Pandemic

Liang Tian^{1,2,#}, Xuefei Li^{1,3,#}, Fei Qi^{1,3}, Qian-Yuan Tang^{1,4}, Viola Tang^{1,5}, Jiang Liu^{1,6}, Zhiyuan Li^{1,7}, Xingye Cheng^{1,2}, Xuanxuan Li^{1,8,9}, Yingchen Shi^{1,8,9}, Haiguang Liu^{1,9,10}, Lei-Han Tang^{1,2,9,*}

#Contributed equally

¹COVID-19 Modelling Group, Hong Kong Baptist University, Kowloon, Hong Kong SAR, China, <http://covid19group.hkbu.edu.hk>

²Department of Physics and Institute of Computational and Theoretical Studies, Hong Kong Baptist University, Kowloon, Hong Kong SAR, China

³CAS Key Laboratory of Quantitative Engineering Biology, Shenzhen Institute of Synthetic Biology, Shenzhen Institutes of Advanced Technology, Shenzhen 518055, China

⁴Center for Complex Systems Biology, Universal Biology Institute, University of Tokyo, 113-0033 Tokyo, Japan

⁵Department of Information Systems, Business Statistics and Operations Management, Hong Kong University of Science and Technology, Hong Kong SAR, China

⁶Scarsdale, NY 10683, USA

⁷Center for Quantitative Biology, Peking University, Haidian, Beijing 100871, China

⁸Department of Engineering Physics, Tsinghua University, Haidian, Beijing 100084, China

⁹Complex Systems Division, Beijing Computational Science Research Center, Haidian, Beijing 100193, China

¹⁰Physics Department, Beijing Normal University, Haidian, Beijing 100875, China

*Correspondence: lhtang@hkbu.edu.hk, Lei-Han Tang, Department of Physics, Hong Kong Baptist University, Hong Kong SAR, China

Abstract

COVID-19 has infected more than 823,000 people globally and resulted in over 40,000 deaths as of April 1, 2020. Swift government response to contain the outbreak requires accurate and continuous census of the infected population, particularly with regards to viral carriers without severe symptoms. We take on this task by converting the symptom onset time distribution, which we calibrated, into the percentage of the latent, pre-symptomatic and symptomatic groups through a novel mathematical procedure. We then estimate the reduction of the basic reproduction number R_0 under specific disease control practices such as contact tracing, testing, social distancing, wearing masks and staying at home. When these measures are implemented in parallel, their effects on R_0 multiply. For example, if 70% of the general public wear masks and contact tracing is conducted at 60% efficiency within a 4-day time frame, epidemic growth will be flattened in the hardest hit countries. Finally, we analyze the bell-shaped curves of epidemic evolution from various affected regions and point out the significance of a universal decay rate of $-0.32/\text{day}$ in the final eradication of the disease.

Keywords: COVID-19, Disease transmission model, Pre-symptomatic, Epidemic evolution and control.

The Coronavirus Disease 2019 (COVID-19) is a new contagious disease caused by the novel coronavirus (SARS-COV-2) (1), which belongs to the genera of *betacoronavirus*, the same as the coronavirus that caused the SARS epidemic between 2002 and 2003 (2). COVID-19 has spread to more than 170 countries, infected more than 823,000 people and claimed over 40,000 lives as of April 1, 2020 (3). The outbreak has been declared a pandemic and a public health emergency of international concern (4). Given its enormous span over a great variety of communities and nations, data from all sources are needed to formulate successful intervention strategies towards the containment of the disease. At this stage, there exists a wealth of carefully documented clinical data on disease progression and transmission, which can be mined to construct quantitative models of how individual outbreaks rise and cede. Coupled with a systematic characterization of how the disease has spread within and among different communities, a basket of intervention measures can be identified and assessed against the associated economic and social costs.

As the specific symptoms of COVID-19 are now well-publicized, symptomatic transmissions are being contained in most countries. However, disease transmission by pre-symptomatic and asymptomatic viral carriers is much harder to deal with due to its hidden nature (5). Clinical data reveals that viral load becomes significant before the symptom onset (6–8). The epidemiological investigation has identified cases of pre-symptomatic transmission based on the onset time interval studies (9–12). Estimates vary greatly among experts on the percentage of total transmission due to this group of viral carriers, ranging from as low as 18% to over 50% (13–15). A model-based study by Ferretti *et al.* (16) suggested that pre-symptomatic transmission alone could yield a basic reproduction number $R_{0,p} = 0.9$, close to the critical value of 1.0 that sustains epidemic growth. As the epidemic is driven by the most infectious group at any given period, it is not inconceivable that, as symptomatic transmission loses heat, pre-symptomatic and asymptomatic transmission takes over in fueling the outbreak (5).

To tackle the myriad of issues and questions regarding the outbreak, a simple quantitative model, based on the clinical facts of COVID-19 transmission, is much desired. The model can provide a timely assessment of current intervention measures and of new policies to change the course of the pandemic. In this paper, we show that such a goal is indeed reachable. By transforming the symptom onset time distribution into the reproductive rate since infection, we build a quantitative model that brings out universal features of individual outbreaks. The model allows one to convert the cumulative number of confirmed cases to the current size of the pre-symptomatic population. Subsequently, one can estimate the percentage reduction in the basic reproduction number R_0 (estimated to be around 3.68 at a growth rate of

0.3/day) due to contact tracing, wearing masks and other additional measures, individually or in combination. Additionally, we present our findings against the epidemic development curves around the world to highlight the level of social mobilization required to prevent COVID-19 from spreading further.

Model

In epidemiological studies, the central quantity is the average number of infections per unit time $r(t)$ by a viral carrier who was infected at $t = 0$ (17, 18). In the case of COVID-19, disease transmission by a given individual peaks around his/her symptom onset time (7, 8), as illustrated by the infectiousness curve shown in Fig. 1. This property, when averaged over the population, gives an $r(t)$ that peaks at nearly the same time as the symptom onset time distribution, which we denote by $p_O(t)$. In fact, when the time window of transmission is narrow compared to the mean symptom onset time τ_O , we have approximately

$$r(t) \approx R_0 p_O(t). \quad (1)$$

Equation (1) forms the basis of our analysis. Throughout this paper, we shall use R_0 to denote the mean number of secondary infections per infected individual in the population considered.

To incorporate the actual shape of the infectiousness curve, we developed a more complete model as presented in Supplementary Materials (SM). The model splits the pre-symptomatic period into two phases, a non-infectious latent phase L, followed by the infectious pre-symptomatic phase A. As usually done in SEIR type models (19), the infected population is grouped by the symptom phases, denoted as L, A, and S, except that a non-Markovian formulation is required here to accommodate an arbitrary onset time distribution. Starting from infection at $t = 0$, an individual first stays in the latent phase L. Transition to phase A takes place at a rate $\alpha_L(t)$, which increases with t . After some time in phase A, the individual develops symptoms and enters the symptomatic S phase at a rate α_A , independent of how long the person has been in phase A. The mean duration of phase A is given by α_A^{-1} , chosen to correspond to the size of the left-wing of the infectiousness curve. The transmission rate in phase A is set by β_A . Once in S, the person remains in this phase and the subsequent disease development is not followed. Disease transmission rate $\beta_S(\tau)$ is a function of $\tau = t - t_O$ that matches the right-wing of the infectiousness curve. The total area underneath the infectiousness curve is given by $R_0 = R_0^A + R_0^S$, with $R_0^A = \beta_A/\alpha_A$, and $R_0^S = \int_0^\infty \beta_S(\tau)d\tau$. Introducing a parameter $\beta_{\text{eff}} = \beta_A + \alpha_A R_0^S$, we have

$$R_0 = \frac{\beta_{\text{eff}}}{\alpha_A}. \quad (2)$$

This completes the specification of our detailed model. In SM, we show that the $r(t)$ of this model can be written in the form of Eq. (1) with a slightly modified onset time distribution. In view of its mathematical simplicity, we will adopt Eq. (1) in the

following and leave the more technical discussions to SM. Denoting by $A(t)$ the size of the infected population in phase A in a well-mixed community, we have

$$\dot{A} = -\alpha_A A + \int_{-\infty}^t K(t-t_1)A(t_1)dt_1, \quad (3)$$

with the kernel function given by

$$K(t) = R_0 e^{-\alpha_A t} \frac{d}{dt} [e^{\alpha_A t} p_O(t)]. \quad (4)$$

An obvious advantage of our formulation, as compared to the more traditional approaches (16, 20–22), is that its parameters have clear physical meaning and thus can be determined directly from clinical case studies. We undertake this task below using available data. By combining two data sets (11, 23) with a total of 159 infection cases, we calibrated the statistical behavior of the symptom onset time as shown in Fig. 2a, and obtained a mean value $\tau_O = 5.17$ days, with a standard deviation of 2.93 days. The data is validated against a serial interval study on 468 infection pairs (9) with excellent consistency (see SM). Starting from day 6, $p_O(t)$ decays exponentially at a rate of $-0.32/\text{day}$. As will be elaborated later, this decay rate is also seen in the decreasing rate of daily cases when the infectious population is fully isolated and can be attributed to the statistics of the latent period t_L . The parameter α_A controls the apparent duration of phase A, but its actual value has only a weak effect on our predictions. In our numerical exploration, we use the estimated value $\alpha_A \approx 0.75/\text{day}$ based on a data set compiled by Xia *et al.* (11). The basic reproduction number R_0 reflects the regional social contact pattern in a specific period.

Figure 2b shows the probabilities that a given individual is in one of the three phases at day t after infection, computed using the formula in Table S1 (SM). The red line marks the boundary between the pre-symptomatic and symptomatic phases. Dashed lines above the red line indicate probabilities that the individual is one day or two days into the symptomatic phase, respectively. The width of the orange region, on the other hand, is proportional to $\alpha_A^{-1} = 1.5$ days.

Figure 2c, obtained from the Laplace transforms of these curves, gives the percentage of the infected population in each of the three phases on a given day when the epidemic is growing at a rate λ . These curves allow for estimation of the hidden population in L and A from the knowledge of S in real-time and form the basis for quantitative assessment of intervention measures. The actual size of S, which includes all individuals who have developed symptoms in the past, regardless of whether they have recovered from the disease, can be estimated from the total number of confirmed cases until that time point. Note that at high growth rates, probabilities at short times in Fig. 2b contribute more to the Laplace transforms, leading to a larger percentage of the total infectious population being constituted by the hidden population.

Under Eq. (1), the well-known Lotka–Euler estimating equation (24) yields,

$$R_0 = \frac{1}{\tilde{p}_O(\lambda)}, \quad (5)$$

where $\tilde{p}_O(\lambda) = \int_0^\infty p_O(t)e^{-\lambda t} dt$ is the Laplace transform of $p_O(t)$. Using our calibrated numbers, we obtain from Eq. (5) the R_0 - λ curve shown in Fig. 2d for COVID-19, which covers both growth and decline phases of the epidemic. The slope of the curve at $R_0 = 1$ is given by $1/T_g$, where T_g is the mean generation time and equals $\tau_O = 5.17$ days under Eq. (1) (see Fig. 2a). At the very high growth rate of $\lambda = 0.3/\text{day}$ seen in China in late January 2020 and now in Europe and the US in March 2020, our estimated value of R_0 is 3.68. According to Eq. (2), R_0 is proportional to the transmission parameter β_{eff} . Thus if one is to rely on social distancing alone, the number of close social contacts per individual needs to be reduced to 27% of its original level to reach $R_0 = 1.0$ so as to halt exponential growth, highlighting the tremendous sacrifice required to curb a rapidly growing outbreak. The left end of the curve gives an ultimate epidemic decay rate of $-0.32/\text{day}$ at $R_0 = 0$, i.e., a complete eradication of disease transmission.

Evaluation of Intervention Measures

To lessen the impact of social distancing practices on the general public, governments have mainly adopted two measures to track COVID-19 transmission: 1) testing and isolating infected individuals; and 2) tracing and quarantining contacts of infected individuals. For testing control, persons who had close contact with a confirmed infection case are asked to undergo voluntary or mandatory testing for infection, and quarantined when the result is positive. From Fig. 2b we see that, if the test is conducted too close to the day of infection, the individual has a high probability to still be in the latent phase, hence the test result is likely to be negative. On the other hand, if the test is conducted too late, the person may have already infected others so that the reduction of $r(t)$ given by Eq. (1) is small. Therefore, there is an optimal interval between infection date and the test date, which we analyzed in SM. Figure 3a shows the function $g(t) = r(t)/R_0$ without intervention, and in three examples when the test was performed on day 2, day 3 and day 4 after infection, under the best-case scenario when all close contacts were traced and test results were immediately available. Relative change of the basic reproduction number R_0 is given by the sandwiched area in each case. In Fig. 3b, we show the reduction of R_0 as a function of the test date after infection for immediate reporting (red line) and delay of result by one day (blue line), with an initial value of $R_0 = 3.68$. The best result is obtained when the test is performed on day 4. This corresponds to the day when the width of the orange region in Fig. 2b is the widest. The actual values depend on the total width of the infectious interval, which should also extend to the symptomatic side if self-quarantine is not assumed.

For contact tracing and quarantining, we show our results for aggressive contact tracing under the scenario that all close contacts are traced and quarantined on day t after infection, without testing the individual for the virus (Fig. 3b). The reduction of R_0 is much greater if full tracing and quarantining are executed within 2-3 days

after infection. An 80% tracing efficiency shrinks the time window to 1 day for achieving the same effect. The above estimation procedure can be generalized to cases when testing or contact tracing is completed within a given period rather than on a particular day in terms of a weighted average of the reductions (see SM). These numbers can be used to design optimal strategies that combine social distancing, testing and contact tracing to contain the epidemic in a particular region, taking into account the local political, economic and social situations.

Other than government-led intervention, individual-led interventions, including social-distancing, mask-wearing, frequent hands washing, etc., may reduce disease transmission and slow down the outbreak. Among them, population-wide mask wearing is currently under debate (25). It is enforced in most Asian countries, but not recommended by the CDCs in the EU and USA as of 31 March, 2020. Given the now established risk of pre-symptomatic transmission, and the dominant role of droplet-mediated COVID-19 infections (26), masks with relatively low efficacy for personal protection may nevertheless reduce the overall infections in a population (27). Based on a previous study on influenza aerosols (28), we constructed a semi-quantitative model to show that mask-wearing reduces β_{eff} and hence R_0 by a factor $(1 - e \cdot p_m)^2$, where e is the efficacy of trapping viral particles inside the mask, and p_m is the percentage of mask-wearing population (see SM). According to this model, mask-wearing at 96% alone could flatten an epidemic growing at a rate of 0.3/day by bringing down R_0 from its original value of 3.68 to 1. When combined with contact tracing (Fig. 3b), the two effects multiply. Figure 3c shows a heatmap of the reduced R_0 when contact tracing and isolation is completed within 4 days of infection. The solid yellow line indicates that the reduced R_0 reaches 1. For example, the combination of tracing of close contacts at 60% efficiency within 4 days and 70% of the general public wearing masks achieves the same purpose. This target line can be reached with lower percentages when close contacts can be found within 2 days of possible infection (red dashed line), but the numbers need to be higher when the time frame is relaxed to 7 days (green dashed line).

Three-phase Epidemic Development

From the time-series data of daily confirmed cases of COVID-19 obtained from the Johns Hopkins CSSE Repository (29), we identify three phases of COVID-19 epidemic development from different places in China following the Wuhan lockdown on January 23, 2020, with universal features at the beginning and end of regional outbreaks. These observations are interpreted within our model setting.

Phase I is characterized by exponential growth of the epidemic. In China, in the first week after the Wuhan lockdown on January 23, 2020, the number of daily confirmed cases continued to grow at a rate of approximately 0.3/day (Fig. 4a and 4b, dashed-black line), equivalent to an eight-fold increase per week. Data shows that most of the growth during this period is related to infections that can be traced to Hubei province, the epicenter of the initial outbreak. As we explain in the SM, the universal growth rate is set by latent, pre-symptomatic and symptomatic viral carriers from Hubei province, whose percentage among these travelers, while still low,

grows exponentially in that period. The fraction of local infections can be calculated using our model, and the result depends on the local value of R_0 .

Phase II is a crossover phase where public policies on border control and to contain the disease spreading are taking effect. On a logarithmic scale, data from the most affected provinces apart from Hubei show consistent behavior. Close examination, however, reveals sporadic outbreaks in local communities that vary from province to province. Well-known examples include prison cases in Hubei, Shandong and Zhejiang provinces (30). Overall, under the swift and forceful implementation of contact tracing, isolation and social distancing policies, turnaround of the epidemic in provinces other than Hubei was reached in about three weeks after the regional lockdown. In Fig. 4b and the supplementary Fig. S5, we present simulation results using our model, assuming a linear decrease of R_0 from a local value of 2.0 to zero over a period T , which indeed reproduces the bell-shaped curve as seen in Fig. 4. The more gradual change of R_0 assumed in our simulations can be interpreted as due to the progressive government policies including additional lockdowns, which took place from February 4-10 (31, 32), as well as the time needed for these policies to take effect in communities that experienced new outbreaks.

Phase III, or the final descent, occurred when the intervention measures essentially eliminated new outbreaks. The few that surfaced were quickly identified and contained. Within our model, the newly confirmed cases in this period are identified with the shrinking number of individuals moving from the latent to the symptomatic phase, as one moves along the time axis in Fig. 2b. Strikingly, the observed decay rate in this phase reached the maximum value of 0.32/day, including data from Hubei province shown in Fig. 4a. This observation indicates that the infected cases were isolated at extremely high efficiency.

We now examine the situation elsewhere in the world. Exponential growth with a daily growth rate of around 0.3 is seen in the latest epidemic data from a number of countries (Fig. 4c). While these outbreaks were initially seeded by imported cases, they are now largely driven by local infections. Under successful interventions, a few countries have transitioned to the crossover phase observed in China in February (Fig. 4d). The government of Italy imposed a national quarantine on March 9 (33), after which growth in the number of newly confirmed cases slowed down (29). On the other hand, South Korea adopted very aggressive contact tracing and testing policies (34, 35), enabling the country to bring the initially rampaging outbreak to a much more manageable level at $R_0 \approx 1$ (Fig. 4d, stars). These countries are now facing the challenge of dealing with import driven growth, which can be analyzed using our model (see SM).

Conclusions

We have developed a simple yet powerful model to describe the spread of COVID-19 infection, which can be applied to communal outbreaks. The effect of intervention measures in a regional or national setting, such as border closing, social distancing, contact tracing, testing, quarantining and mask wearing, can be readily incorporated

into the model for quantitative assessment and prediction. In the ongoing battle in many countries, further reduction of the still positive growth rate requires quantitative evaluation of the proposed measures. While the data used to construct the reproduction rate function given by Eq. (1) will continue to be updated, our current predictions should already be informative to decision-makers. As the pandemic is fueled by transmission in the fastest growing community, reaching out to all sectors of society will pose the biggest challenge. In this respect, comprehensive monitoring of the pandemic development will be essential.

An important issue not treated explicitly in this work is the role played by asymptomatic carriers of the virus, i.e., those who never exhibit severe symptoms. We have made the implicit but plausible assumption that the reproduction rate function for this group of infected individuals is weaker or the same as the one given by Eq. (1), in which case their contribution is slaved to the group captured by Eq. (3), without altering the main structure of our model. We would like to emphasize that transmission by both pre-symptomatic and asymptomatic viral carriers can be much reduced under strict enforcement of social distancing and staying at home regulations in combination with wearing masks in public places, particularly when available resources and infrastructure do not allow for robust implementation of contact tracing and testing within the required time frames.

Acknowledgments

The work is supported in part by the NSFC under Grant Nos. 11635002 and U1530402, and by the Research Grants Council of the Hong Kong Special Administrative Region (HKSAR) under Grant Nos. HKBU 12324716.

Conflict of Interest Statement

Authors declare no conflict of interest.

Disclaimer

Any views expressed by Jiang Liu and Viola Tang are not as a representative speaking for or on behalf of his/her employer, nor do they represent his/her employer's positions, strategies or opinions.

References

1. P. Zhou, X. Lou Yang, X. G. Wang, B. Hu, L. Zhang, W. Zhang, H. R. Si, Y. Zhu, B. Li, C. L. Huang, H. D. Chen, J. Chen, Y. Luo, H. Guo, R. Di Jiang, M. Q. Liu, Y. Chen, X. R. Shen, X. Wang, X. S. Zheng, K. Zhao, Q. J. Chen, F. Deng, L. L. Liu, B. Yan, F. X. Zhan, Y. Y. Wang, G. F. Xiao, Z. L. Shi, A

- pneumonia outbreak associated with a new coronavirus of probable bat origin. *Nature*. **579**, 270–273 (2020).
2. F. Wu, S. Zhao, B. Yu, Y. M. Chen, W. Wang, Z. G. Song, Y. Hu, Z. W. Tao, J. H. Tian, Y. Y. Pei, M. L. Yuan, Y. L. Zhang, F. H. Dai, Y. Liu, Q. M. Wang, J. J. Zheng, L. Xu, E. C. Holmes, Y. Z. Zhang, A new coronavirus associated with human respiratory disease in China. *Nature*. **579**, 265–269 (2020).
 3. World Health Organization, “Coronavirus disease 2019 (COVID-19) Situation Report -72” (2020), (available at https://www.who.int/docs/default-source/coronaviruse/situation-reports/20200401-sitrep-72-covid-19.pdf?sfvrsn=3dd8971b_2).
 4. W. World Health Organization, WHO Director-General’s opening remarks at the media briefing on COVID-19 - 11 March 2020. *WHO Dir. Gen. speeches* (2020), p. 4.
 5. R. M. Anderson, H. Heesterbeek, D. Klinkenberg, T. D. Hollingsworth, How will country-based mitigation measures influence the course of the COVID-19 epidemic? *Lancet*. **395** (2020), pp. 931–934.
 6. L. Zou, F. Ruan, M. Huang, L. Liang, H. Huang, Z. Hong, J. Yu, M. Kang, Y. Song, J. Xia, Q. Guo, T. Song, J. He, H.-L. Yen, M. Peiris, J. Wu, SARS-CoV-2 Viral Load in Upper Respiratory Specimens of Infected Patients. *N. Engl. J. Med.* (2020), doi:10.1056/NEJMc2001737.
 7. X. He, E. H. Lau, P. Wu, X. Deng, J. Wang, X. Hao, Y. C. Lau, J. Y. Wong, Y. Guan, X. Tan, X. Mo, Y. Chen, B. Liao, W. Chen, F. Hu, Q. Zhang, M. Zhong, Y. Wu, L. Zhao, F. Zhang, B. J. Cowling, F. Li, G. M. Leung, *medRxiv*, in press, doi:10.1101/2020.03.15.20036707.
 8. K. K. To, O. Tak, Y. Tsang, W. Leung, A. R. Tam, T. Wu, D. C. Lung, C. C. Yip, J. Cai, J. M. Chan, T. S. Chik, D. P. Lau, C. Y. Choi, L. Chen, W. Chan, K. Chan, J. D. Ip, A. C. Ng, R. W. Poon, C. Luo, V. C. Cheng, J. F. Chan, I. F. Hung, Z. Chen, H. Chen, K. Yuen, F. Richard, C. Yu, M. Tam, M. Mei, T. Shaw, F. Hong, M. Tong, M. Lee, Articles Temporal profiles of viral load in posterior oropharyngeal saliva samples and serum antibody responses during infection by SARS-CoV-2 : an observational cohort study. *Lancet Infect. Dis.* **3099**, 1–10 (2020).
 9. Z. Du, X. Xu, Y. Wu, L. Wang, B. J. Cowling, L. A. Meyers, *medRxiv*, in press, doi:10.1101/2020.02.19.20025452.
 10. H. Nishiura, N. M. Linton, A. R. Akhmetzhanov, Serial interval of novel coronavirus (COVID-19) infections. *Int. J. Infect. Dis.* **93**, 284–286 (2020).
 11. W. Xia, J. Liao, C. Li, Y. Li, X. Qian, X. Sun, H. Xu, G. Mahai, X. Zhao, L. Shi, J. Liu, L. Yu, M. Wang, Q. Wang, A. Namat, Y. Li, J. Qu, Q. Liu, X. Lin, S. Cao, S. Huan, J. Xiao, F. Ruan, H. Wang, Q. Xu, X. Ding, X. Fang, F. Qiu, J. Ma, Y. Zhang, A. Wang, Y. Xing, S. Xu, *medRxiv*, in press, doi:10.1101/2020.03.06.20031955.
 12. R. Huang, J. Xia, Y. Chen, C. Shan, C. Wu, A family cluster of SARS-CoV-2 infection involving 11 patients in Nanjing, China. *Lancet Infect. Dis.* **0** (2020),

- doi:10.1016/s1473-3099(20)30147-x.
13. K. Mizumoto, K. Kagaya, A. Zarebski, G. Chowell, Estimating the asymptomatic proportion of coronavirus disease 2019 (COVID-19) cases on board the Diamond Princess cruise ship, Yokohama, Japan, 2020. *Eurosurveillance*. **25**, 2000180 (2020).
 14. Y. Dong, X. Mo, Y. Hu, X. Qi, F. Jiang, Z. Jiang, S. Tong, Epidemiological Characteristics of 2143 Pediatric Patients With 2019 Coronavirus Disease in China. *Pediatrics* (2020), doi:10.1542/peds.2020-0702.
 15. H. Wang, Z. Wang, Y. Dong, R. Chang, C. Xu, X. Yu, S. Zhang, L. Tsamlag, M. Shang, J. Huang, Y. Wang, G. Xu, T. Shen, X. Zhang, Y. Cai, Phase-adjusted estimation of the number of Coronavirus Disease 2019 cases in Wuhan, China. *Cell Discov.* **6**, 10 (2020).
 16. L. Ferretti, C. Wymant, M. Kendall, L. Zhao, A. Nurtay, D. G. Bonsall, C. Fraser, *Science.*, in press, doi:10.1126/science.abb6936.
 17. C. Fraser, S. Riley, R. M. Anderson, N. M. Ferguson, Factors that make an infectious disease outbreak controllable. *Proc. Natl. Acad. Sci. U. S. A.* **101**, 6146–6151 (2004).
 18. N. C. Grassly, C. Fraser, Mathematical models of infectious disease transmission. *Nat. Rev. Microbiol.* **6** (2008), pp. 477–487.
 19. N. G. Becker, T. Britton, Statistical studies of infectious disease incidence. *J. R. Stat. Soc. Ser. B Stat. Methodol.* **61**, 287–307 (1999).
 20. A. J. Kucharski, T. W. Russell, C. Diamond, Y. Liu, J. Edmunds, S. Funk, R. M. Eggo, F. Sun, M. Jit, J. D. Munday, N. Davies, A. Gimma, K. van Zandvoort, H. Gibbs, J. Hellewell, C. I. Jarvis, S. Clifford, B. J. Quilty, N. I. Bosse, S. Abbott, P. Klepac, S. Flasche, *Lancet Infect. Dis.*, in press, doi:10.1016/s1473-3099(20)30144-4.
 21. J. M. Read, J. R. R. E. Bridgen, D. A. T. A. Cummings, A. Ho, C. P. Jewell, Novel coronavirus 2019-nCoV: early estimation of epidemiological parameters and epidemic predictions. *medRxiv* (2020), doi:10.1017/CBO9781107415324.004.
 22. M. Chinazzi, J. T. Davis, M. Ajelli, C. Gioannini, M. Litvinova, S. Merler, A. Pastore Y Piontti, K. Mu, L. Rossi, K. Sun, C. Viboud, X. Xiong, H. Yu, M. E. Halloran, I. M. Longini, A. Vespignani, The effect of travel restrictions on the spread of the 2019 novel coronavirus (COVID-19) outbreak. *Science.* (2020), doi:10.1126/science.aba9757.
 23. K. Men, X. Wang, Y. Li, G. Zhang, J. Hu, Y. Gao, H. Han, Estimate the incubation period of coronavirus 2019 (COVID-19). *medRxiv* (2020), doi:10.1101/2020.02.24.20027474.
 24. J. Wallinga, M. Lipsitch, How generation intervals shape the relationship between growth rates and reproductive numbers. *Proc. R. Soc. B Biol. Sci.* **274**, 599–604 (2007).
 25. K. Servick, Would everyone wearing face masks help us slow the pandemic? *Science.* (2020), doi:10.1126/science.abb9371.
 26. World Health Organization, Modes of transmission of virus causing COVID-19: implications for IPC precaution recommendations (2020), (available at

- <https://www.who.int/news-room/commentaries/detail/modes-of-transmission-of-virus-causing-covid-19-implications-for-ipc-precaution-recommendations>).
27. M. Face, M. Materials, Standard Test Method for Evaluating the Bacterial Filtration Efficiency (BFE) of Medical Face Mask Materials , Using a Biological Aerosol of. *i* (2001), pp. 1–5.
 28. D. K. Milton, M. P. Fabian, B. J. Cowling, M. L. Grantham, J. J. McDevitt, Influenza Virus Aerosols in Human Exhaled Breath: Particle Size, Culturability, and Effect of Surgical Masks. *PLoS Pathog.* **9** (2013), doi:10.1371/journal.ppat.1003205.
 29. E. Dong, H. Du, L. Gardner, An interactive web-based dashboard to track COVID-19 in real time. *Lancet. Infect. Dis.* **3099**, 19–20 (2020).
 30. CNBC News, China says more than 500 cases of the new coronavirus stemmed from prisons (2020), (available at <https://www.cnbc.com/2020/02/21/coronavirus-china-says-two-prisons-reported-nearly-250-cases.html>).
 31. K. C. Chong, W. Cheng, S. Zhao, F. Ling, K. Mohammad, M. Wang, B. Zee, L. Wei, X. Xiong, H. Liu, J. Wang, E. Chen, *medRxiv*, in press, doi:10.1101/2020.03.15.20036541.
 32. Sina News, Wuhan lockdown (2020), (available at <https://news.sina.com.cn/c/2020-02-15/doc-iimxxstf1526561.shtml>).
 33. NY Post, Italy’s coronavirus lockdown extended to entire country (2020), (available at <https://nypost.com/2020/03/09/italys-coronavirus-lockdown-extended-to-entire-country>).
 34. A. Dudden, A. Marks, South Korea took rapid, intrusive measures against Covid-19 – and they worked | Alexis Dudden and Andrew Marks | Opinion | The Guardian. *Guard.* (2020), (available at <https://www.theguardian.com/commentisfree/2020/mar/20/south-korea-rapid-intrusive-measures-covid-19>).
 35. Observers, Food, water and masks: South Korea’s COVID-19 quarantine kits (2020), (available at <https://observers.france24.com/en/20200305-south-korea-coronavirus-COVID-19-kits-masks>).

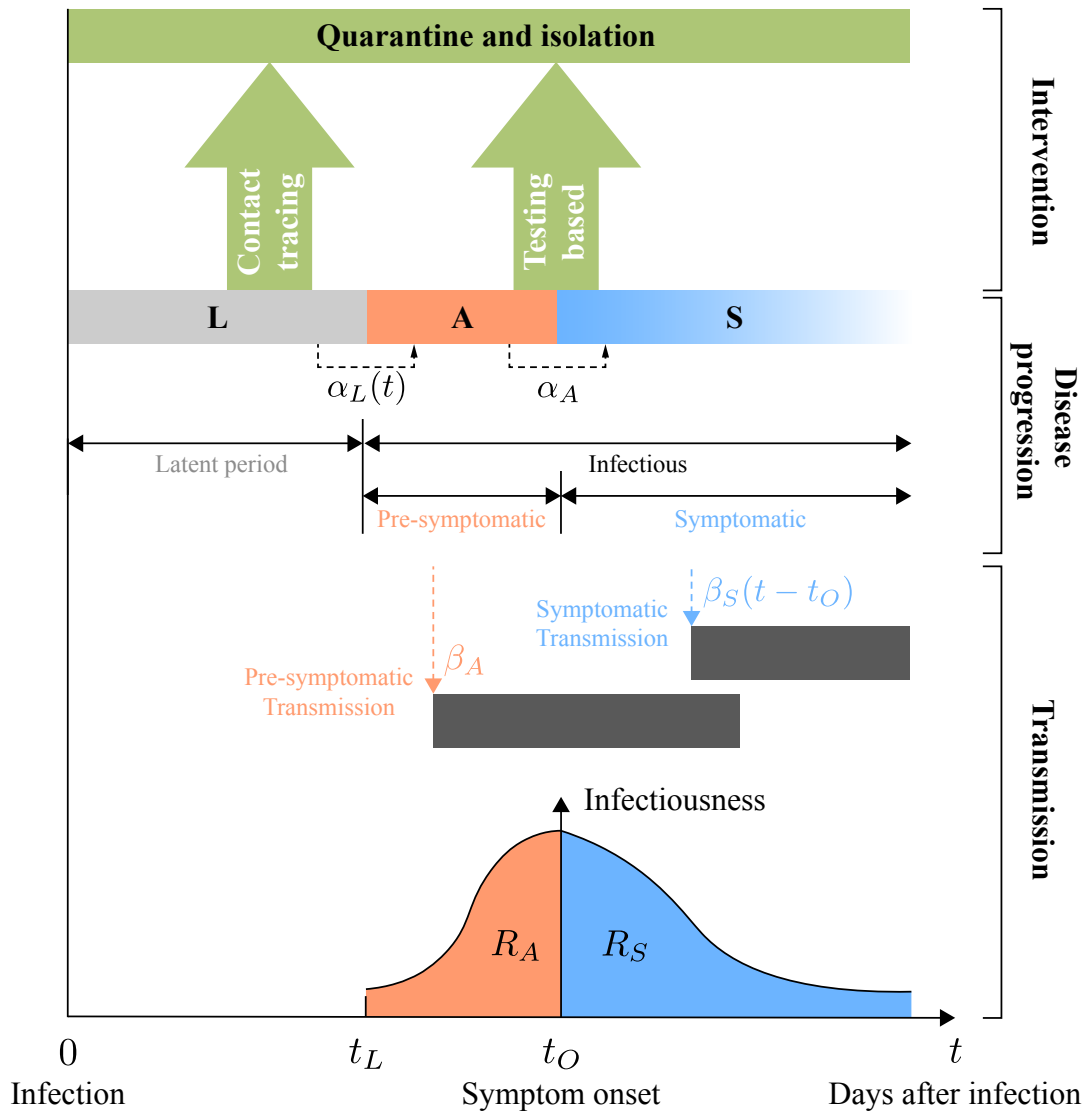


Figure 1. Transmission of COVID-19 during disease progression and intervention. COVID-19 disease progression and transmission: A person infected at time $t = 0$ first goes through a non-infectious latent phase (L) until t_L , marking the start of the infectious period. The infectious period consists of two phases, pre-symptomatic (A) and symptomatic (S). In phase A, the person is infectious without symptoms, during which the virus can be spread through pre-symptomatic transmission (orange dashed arrow). At the symptom onset time t_0 , the person enters the S phase and infects others with symptomatic transmission (blue dashed arrow). The infectiousness of the person peaks around the symptom onset time. The basic reproduction number R_0 is split into R_A and R_S , given by areas underneath the curve on either side of the symptom onset point, respectively. Interventions to limit transmission: contact tracing brings an infected person out of the transmission cycle at the point of isolation, while testing is effective only when the person has developed high viral load and is already in the infectious period.

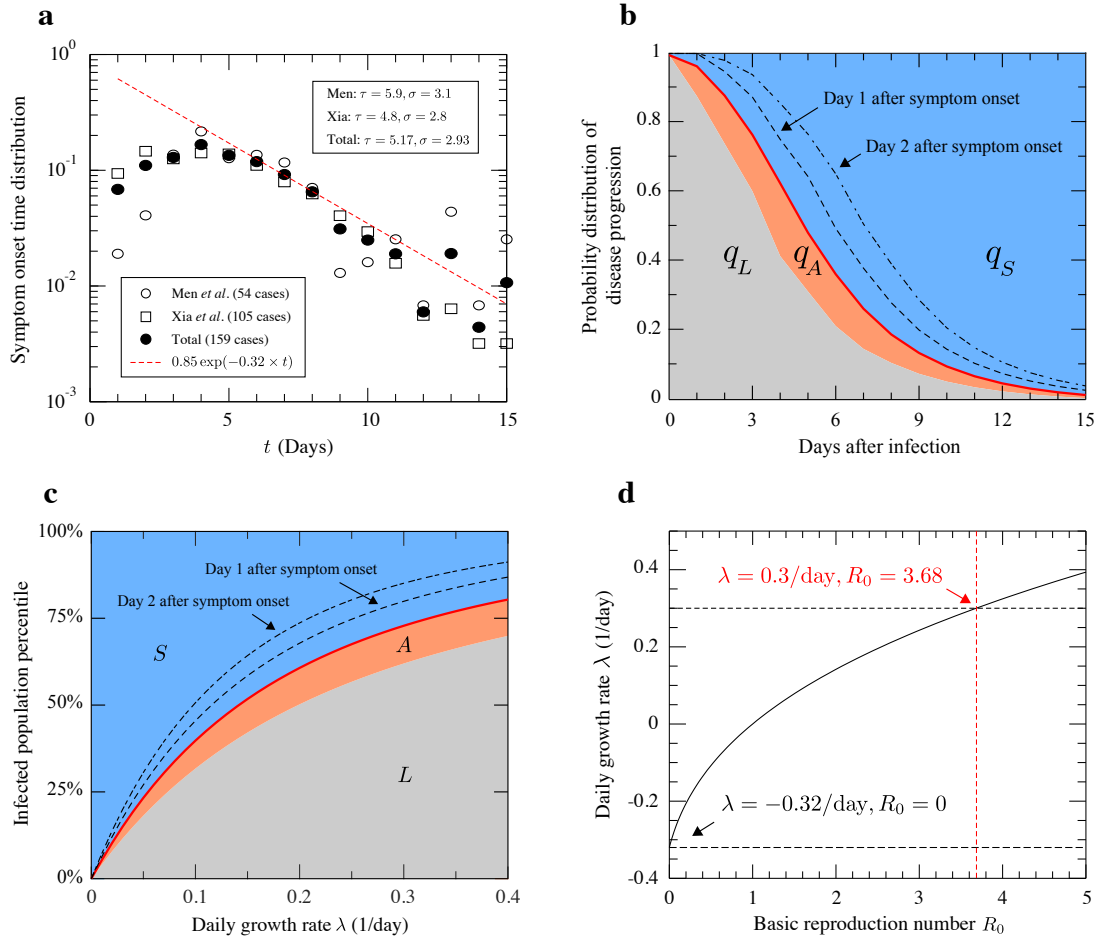


Figure 2. Data and model predictions. **a**, The symptom onset time distribution. Two data sets from previous studies are shown (hollow circles (23) and squares (11)). The mean values and standard deviations are given in the legend. The distribution of the union of the two datasets is shown in solid circles. The red dashed line gives a reference exponential function shown in the legend. **b**, Probabilities for an infected individual being in each of the three phases at day t after infection. The red curve indicates the boundary between the L+A and S phases. The probabilities that an individual is one day or two days into the S phase can be obtained from respective areas bounded by dashed and dashed-dotted curves, respectively. **c**, Percentage of the infected population in each phase when the epidemic is growing at a rate λ . The red curve indicates the boundary between the L+A and S phases. The percentages of the population one day or two days into the S phase are indicated by dashed and dashed-dotted lines, respectively. **d**, The relationship between the growth rate λ and basic reproduction number R_0 . At $\lambda = 0.3$, R_0 is 3.68.

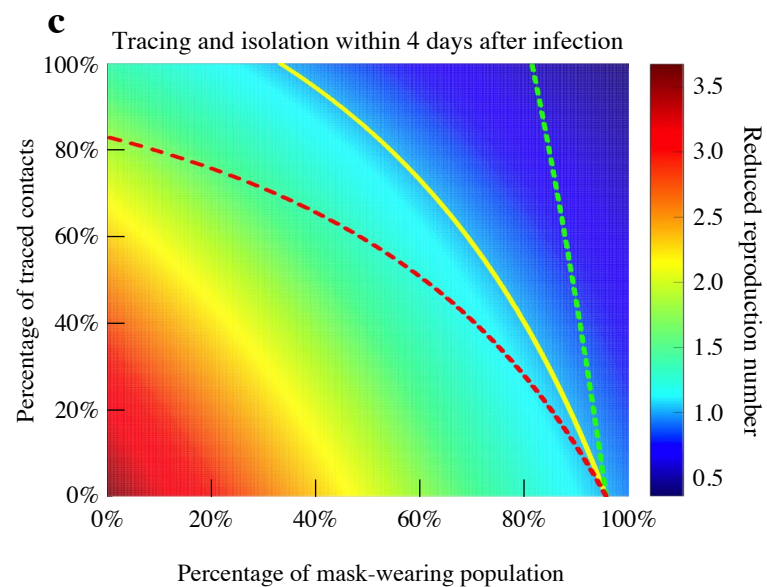
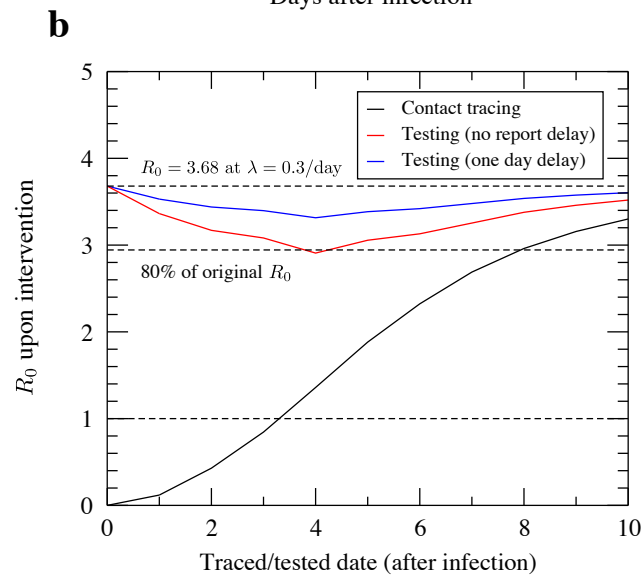
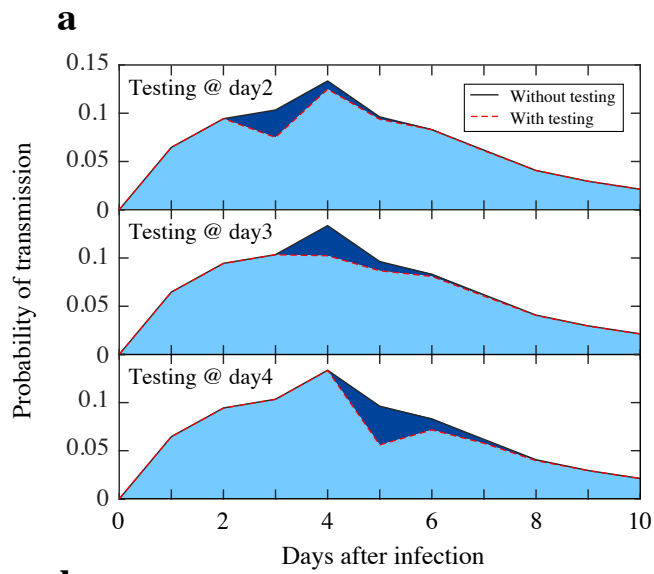


Figure 3. Evaluation of Intervention Measures. **a**, Transmission probability (each day) from our model (black lines) and its revised values (unnormalized) under one-time testing (red dashed lines) performed on day 2 (top), day 3 (middle) and day 4 (bottom) after infection. The basic reproduction number R_0 is given by the area under the curve in each case. **b**, Reduction of the basic reproduction number R_0 against intervention time, calculated from the day of infection. Results are given for contact tracing and isolation (black line), and testing with 0 or 1 day reporting delay (red, blue curves), respectively. The value of R_0 at 3.68 corresponds to a growth rate $\lambda = 0.3$. Time is measured in days. **c**, Reduction of basic reproduction number R_0 under the combined measures of contact tracing and mask-wearing. The heatmap gives the reduced R_0 when close contacts are traced and isolated within 4 days after suspected infection, assuming a basal value of 3.68. The solid yellow line marks the percentages required to flatten the epidemic growth. The red dashed line and the green dashed line map out the percentages when the time frame for contact tracing is reduced to 2 days or relaxed to 7 days, respectively.

Daily Confirmed Cases of COVID-19

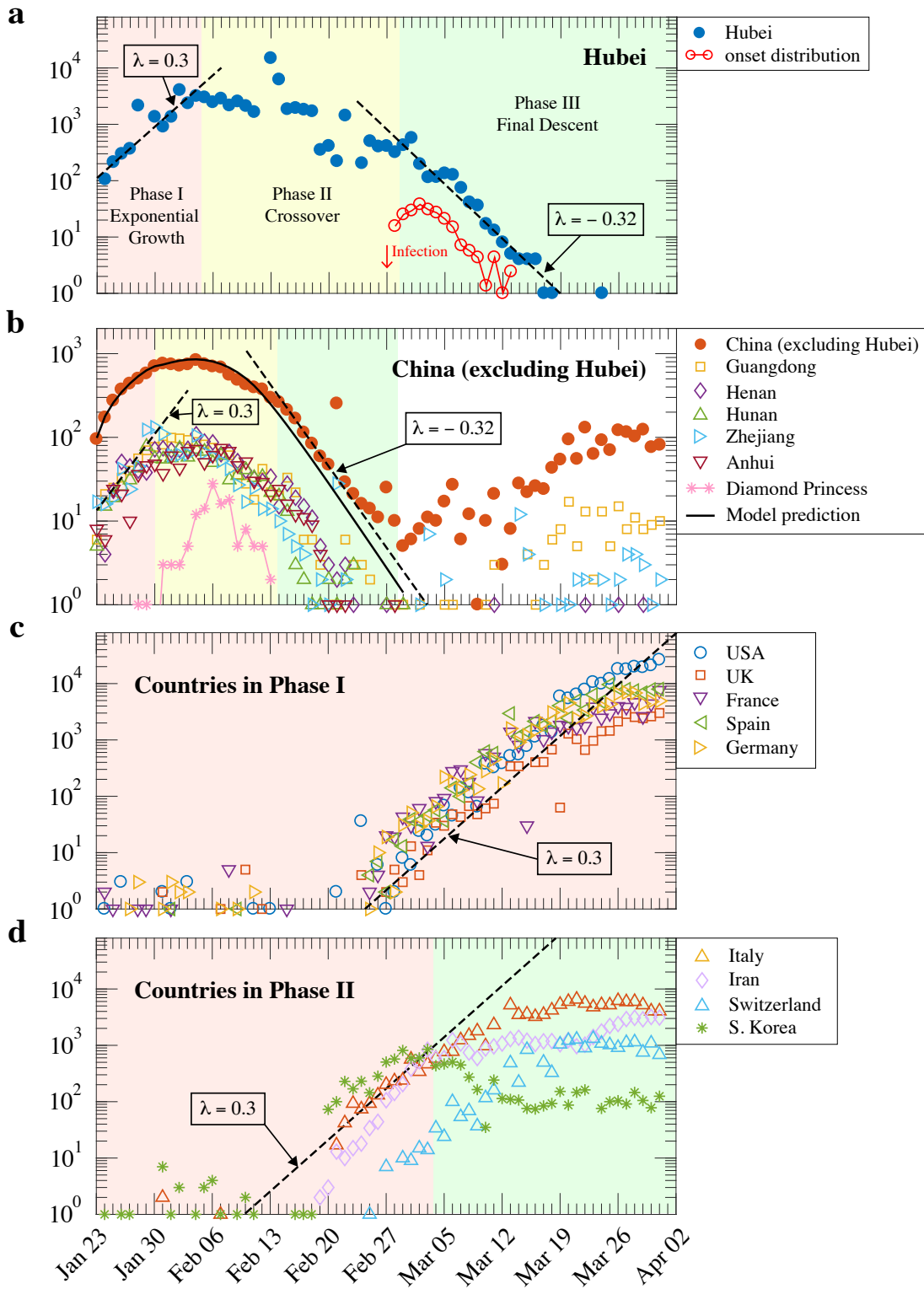


Figure 4. The COVID-19 epidemic development in various countries and regions. Daily confirmed cases in China and other affected countries since the Wuhan lockdown on January 23, 2020. **a**, Hubei province. The three phases of the epidemic development are marked in color: exponential growth (red), crossover

(yellow), and descent phase (green). Early exponential growth reached a rate λ at approximately 0.3/day (left dashed line). Growth slowed and entered the crossover phase in the middle of the second week and reached the third phase nearly four weeks later. The final descent that began in the beginning of March is characterized by $\lambda = -0.32/\text{day}$ (right dashed line). The incubation period distribution is shown in red circles to compare with the exponential decay. **b**, China (excluding Hubei province). The epidemic development in the main affected provinces followed a nearly identical three-phase pattern. Also shown is the model-predicted evolution of the number of daily confirmed cases (solid line), with details given in SM. The increase in the number of newly confirmed cases since the beginning of March is due to imported cases (white region). Data for the Diamond Princess cruise ship is included for comparison. **c**, Countries in phase I. The epidemic progress in these countries is still in the exponential growth phase with a daily rate λ of around 0.3 (dashed line). **d**, Countries entering or in the middle of phase II. Italy, South Korea, and Switzerland have reached zero or negative growth in daily confirmed cases, while data from Iran indicates a slowing down of the exponential growth.